

Army Research Laboratory



**The Atmospheric Sounding Program:
An Analysis and Forecasting Tool for Weather
Hazards on the Battlefield**

By Jeffrey E. Passner

**Information Science and Technology Directorate
Battlefield Environment Division**

19990722 024

ARL-TR-1883

May 1999

Approved for public release; distribution is unlimited.

NOTICES

Disclaimers

The findings in this report are not to be construed as an official Department of the Army position unless so designated by other authorized documents.

Citation of manufacturer's or trade names does not constitute an official endorsement or approval of the use thereof.

REPORT DOCUMENTATION PAGE		Form Approved OMB No. 0704-0188	
Public reporting burden for this collection of information is estimated to average 1 hour per response, including the time for reviewing instructions, searching existing data sources, gathering and maintaining the data needed, and completing and reviewing the collection of information. Send comments regarding this burden estimate or any other aspect of this collection of information, including suggestions for reducing the burden to Washington Headquarters Services, Directorate for Information Operations and reports, 1215 Jefferson Davis Highway, Suite 1204, Arlington, VA 22202-4302 and to the Office of Management and Budget, Paperwork Reduction Project (0704-0188), Washington, DC 20503.			
1. AGENCY USE ONLY (Leave Blank)	2. REPORT DATE May 1999	3. REPORT TYPE AND DATES COVERED Final	
4. TITLE AND SUBTITLE The Atmospheric Sounding Program: An Analysis and Forecasting Tool for Weather Hazards on the Battlefield		5. FUNDING NUMBERS	
6. AUTHOR(S) J. Passner			
7. PERFORMING ORGANIZATION NAME(S) AND ADDRESS(ES) U.S. Army Research Laboratory Information Science and Technology Directorate Battlefield Environment Division ATTN: AMSRL-IS-EW White Sands Missile Range, NM 88002-5501		8. PERFORMING ORGANIZATION REPORT NUMBER ARL-TR-1883	
9. SPONSORING/MONITORING AGENCY NAME(S) AND ADDRESS(ES) U.S. Army Research Laboratory 2800 Powder Mill Road Adelphi, MD 20783-1145		10. SPONSORING/MONITORING AGENCY REPORT NUMBER ARL-TR-1883	
11. SUPPLEMENTARY NOTES			
12a. DISTRIBUTION/AVAILABILITY STATEMENT Approved for public release; distribution is unlimited.		12b. DISTRIBUTION CODE A	
13. ABSTRACT (Maximum 200 words) To assist the staff weather officer and enhance weather predictions in the battlefield, the Atmospheric Sounding Program (ASP) has been designed to furnish a series of weather outputs with an emphasis on weather hazards such as turbulence, icing, clouds, thunderstorms, and surface visibility. The ASP is initialized by either upper-air observations or output from the Battlescale Forecast Model (BFM). The BFM produces a 24-h forecast; thus, the weather hazard is placed into the database and can be displayed for the 24-h forecast period.			
14. SUBJECT TERMS sounding, hazards, battlefield, model, weather		15. NUMBER OF PAGES 68	
		16. PRICE CODE	
17. SECURITY CLASSIFICATION OF THIS REPORT UNCLASSIFIED	18. SECURITY CLASSIFICATION OF THIS PAGE UNCLASSIFIED	19. SECURITY CLASSIFICATION OF ABSTRACT UNCLASSIFIED	20. LIMITATION OF ABSTRACT SAR

Preface

The Atmospheric Sounding Program (ASP), developed at the U.S. Army Research Laboratory, is part of the U.S. Army Integrated Meteorological System Block II software. Using data obtained through the Automated Weather Distribution System (AWDS), the ASP operates worldwide. The ASP uses raw radiosonde data from the AWDS, as well as output data created by the Battlescale Forecast Model that runs on the Integrated Meteorological System.

This report describes the theoretical and mathematical principles used in the ASP.

Contents

Preface	1
Executive Summary	5
1. Introduction	7
2. Data Input Methods into ASP	9
2.1 <i>Sounding Data Using Radiosondes</i>	9
2.2 <i>Sounding Data from BFM Model Output</i>	10
2.3 <i>Archived Data</i>	11
3. The Data and Quality Control	13
3.1 <i>Quality Control</i>	13
3.2 <i>Missing Data from Sounding</i>	14
3.2.1 Missing Temperature, Dew Point, and Wind Data	14
3.2.2 Missing Height Data	15
3.2.3 Missing Pressure Data	15
3.3 <i>Quality Control of the BFM Output Data</i>	16
4. Stability Analysis from the Sounding Data	17
4.1 <i>Thermodynamic Variables</i>	17
4.1.1 Vapor Pressure Calculation	17
4.1.2 Relative Humidity	18
4.1.3 Convective Condensation Level	18
4.1.4 The Lifted Condensation Level	20
4.1.5 Other Thermodynamic Variables	20
4.2 <i>Calculation of Stability Indices</i>	21
4.2.1 K Index	21
4.2.2 Showalter Index	22
4.2.3 Lifted Index	23
4.2.4 Threat Index (SWEAT)	23
4.2.5 Boyden, S, and Ko Indices	25
4.3 <i>Precipitable Water</i>	26
5. Weather Hazards	27
5.1 <i>Turbulence</i>	29
5.2 <i>Icing</i>	32
5.3 <i>Clouds</i>	34

5.3.1 Ceilings and Relative Humidity Study	35
5.3.2 Relative Humidity Values	36
5.4 Thunderstorms	41
5.4.1 Thunderstorm Probability	42
5.4.2 Thunderstorm Severity	44
5.4.2.1 Thunderstorm Gusts	44
5.4.2.2 Thunderstorm Movement	46
5.5 Surface Visibility	46
5.6 Inversion Levels	48
6. Summary	49
References	51
Acronyms and Abbreviations	55
Distribution	57

Figures

1. Skew T-Log T plot from RAOB	9
2. A 12-h forecast skew T-Log P diagram from a BFM run	10
3. Plot of ASP weather hazards based on sounding observation	28

Tables

1. Average relative humidity values (different seasons)	37
2. Average relative humidity values (ceiling heights)	38
3. Difference in BFM output	40

Executive Summary

Introduction

The U.S. Army Research Laboratory, Battlefield Environment Directorate, has developed the Atmospheric Sounding Program (ASP) to assist the Staff Weather Officer in making accurate weather predictions in the battlefield. The ASP is designed to use either conventional upper-air observations from raw input data or output data from the Battlescale Forecast Model (BFM). The output of the ASP is presented in a series of graphic or text packages, which display analyses and forecasts of weather hazards such as icing, turbulence, clouds, reduced surface visibility, and thunderstorm probability.

Purpose

This report describes the data input, the theoretical and mathematical principles used by the ASP, and the different weather hazards that might interfere with military operations. There is a detailed description of stability analyses and many stability indices and how the ASP uses them. Additionally, each weather hazard is described. The techniques used by the ASP to forecast weather hazards give insight into how the routines are developed and utilized.

Overview

The ASP is initialized by upper-air observations, either from standard radiosonde upper-air observations or output from a numerical model, the BFM. These data are decoded and processed before calculations are performed, giving the forecaster an overview of the atmospheric conditions at or near the site of the upper-air data. The ASP uses these data and produces a series of weather hazards that can be used for analyses or forecasts to 24-h from the initial time of the BFM run. Included in these weather hazards are thunderstorm probability, turbulence, icing, clouds, and surface visibility. These meteorological parameters are later entered into a database so that other programs such as the Integrated Weather Effects Decision Aid can investigate how the weather hazards will influence equipment and personnel in the battlefield.

1. Introduction

The Integrated Meteorological System (IMETS) is a mobile operational automated weather data receiving, processing, and disseminating system utilized by Air Force weather forecasters in support of Army operations. The U.S. Army Research Laboratory (ARL) has formulated a number of weather products that will support the forecaster to make more precise and detailed weather decisions. Of most concern to the military is the influence of weather hazards on military operations. These hazards include icing, turbulence, inversion layers, surface visibility, and thunderstorms. Recent efforts have centered on employing sounding data to display text and graphical output of these weather parameters. However, with the development of an operational mesoscale model, the Battlescale Forecast Model (BFM), there has been an effort to make short-term weather forecasts (≤ 24 h) of these weather hazards. [1]

The Atmospheric Sounding Program (ASP) is a program in the IMETS software environment that calculates, interpolates, and displays meteorological data for the forecaster. The program ingests sounding data either from conventional radiosonde data or from 3-D model output. Once these data have been read, the program will process the information and display it so users can make weather decisions. The program displays a skew T-log P diagram, a weather hazards program, and information about thunderstorms and surface visibility. All sounding information, either from the model output or upper-air observations, can be saved and retrieved in the program.

This report is divided into the following sections, each with a different degree of detail.

- Section 1 - Introduction
- Section 2 - Data Input Methods Into ASP
- Section 3 - The Data and Quality Control
- Section 4 - Stability Analysis from The Sounding Data
- Section 5 - Weather Hazards
- Section 6 - Summary

2. Data Input Methods into ASP

Data for the ASP comes from two general sources; either conventional radiosonde data or 3-D output from the BFM. Sounding data is delivered into the IMETS database by either the Automated Weather Distribution System (AWDS), the Automated Weather Network (AWN), or manual input. The latest BFM data is placed into a gridded meteorological database (GMDB), where the ASP can access it.

2.1 Sounding Data Using Radiosondes

This data method uses radiosonde data in World Meteorological Organization (WMO) format. Rawinsonde observations (RAOBS) examine the pressure, temperature, humidity, and wind structure from the earth's surface to where the balloon burst (figure 1). As the balloon rises, these measurements are transmitted to a ground station where data are recorded automatically. These data are commonly divided into different groups known as the TTAAs (mandatory levels), TTBBs (significant-level temperatures), and PPBBs (significant-level winds). The actual number of levels will vary from one rawinsonde report to another. [2]

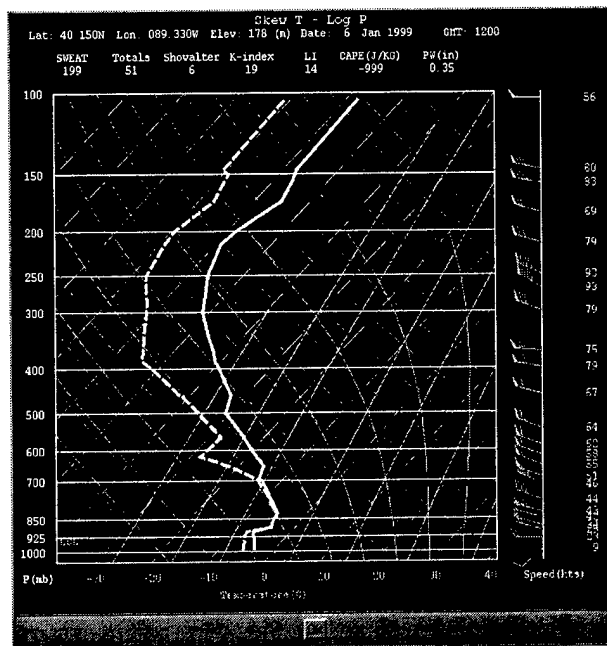


Figure 1. Skew T-Log T plot from RAOB.

2.2 Sounding Data from BFM Model Output

Lee et al. Note that the mesoscale domain can range from 2,000 to 2 km. Of primary interest to the Army is a transitional mesoscale area of 500 km or less, which ARL refers to as the battlescale. With this goal in mind, ARL has adapted a hydrostatic model, Higher Order Turbulence Model for Atmospheric Circulation (HOTMAC), which has been modified for Army applications. [3,4]

One of the main advantages of the BFM is that it takes into account local terrain features, which assist in producing a fine-tuned local forecast (figure 2). By incorporating these local effects in a specific area, the forecaster does not need to be accustomed with the local terrain features that might influence nearby weather patterns. The BFM calculates intercepted solar radiant energy, which can influence localized mesoscale wind fields. It uses the hydrostatic and quasi-Boussinesq approximations and has detailed surface boundary layer physics.

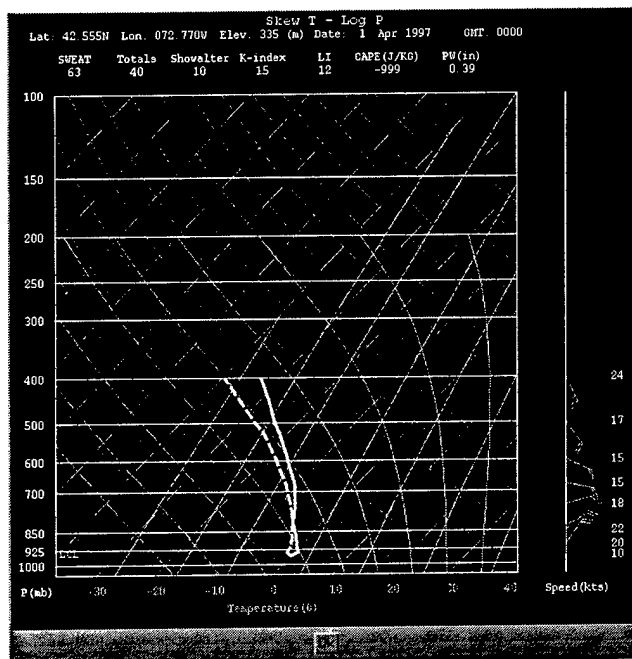


Figure 2. A 12-h forecast skew T-Log P diagram from a BFM run.

BFM initialization includes all observations from the area of interest, such as surface data, upper-air observations, and the 12-h forecasted Naval Operational Global Atmospheric Prediction System (NOGAPS), which is issued by the U.S. Air Force Weather Agency (AFWA) via the Air Force AWDS. The NOGAPS grid points are spaced 381-km (2.5° latitudinal distance) apart on the mandatory pressure surfaces, although integration of grids with 1° resolution will soon be implemented.

Lateral and time-dependent boundary conditions (large-scale forcing) are supplied from grid-point data close to the area of interest. These data are taken from NOGAPS output valid at analysis and forecast times of interest.

The BFM forecast is executed using these boundary conditions and area-of-interest raw data as initialization guidance. It solves towards forecast solutions dictated by global forecast gridded data, although boundary-layer mesoscale flows can be generated when the local terrain and radiation forcing dominate the large-scale forcing.

The main BFM-generated output for the grid include the u and v horizontal wind vector components, potential temperature, and water vapor mixing ratio, where u is the east-west wind component and v is the north-south wind component. These forecast fields are saved at 0-, 3-, 6-, 9-, 12-, 18-, and 24-h from the base time of the model run. Thus, it is possible to manipulate these data at various intervals over the forecast period. A vertical profile of the atmosphere is available at each grid point using these output data.

2.3 Archived Data

The final method of sounding data acquisition is to retrieve past sounding data (from rawinsonde or BFM output) that has been archived in a file on the hard disk.

3. The Data and Quality Control

Prior to processing the data and performing the meteorological calculations, a quality control validation is made of the upper-air sounding data.

3.1 Quality Control

The following procedures are taken to ensure that data received is valid:

1. Check the mandatory-level temperatures and dew points above 500 mb to verify that they are not missing. If they are missing, use the standard-level values.
2. Check the surface layer for missing data. If the surface data is missing, the sounding cannot be used, since interpolation is used for any missing data in the levels above the surface.
3. If both the pressure and height values are missing from a level, eliminate the level.
4. Check each level for inconsistent values. As an example, if the dew point is greater than the temperature value on a level, the dew point and temperature are set as missing and interpolated from surrounding levels.
5. Search each array vertically and fill in missing values of pressure, height, temperature, dew point, wind speed, and wind direction.
6. If there are duplicate levels with the same pressure or heights, eliminate the first one in the list.
7. If a pressure level is ≤ 1 mb from the level below it, eliminate the pressure level since it can cause calculation errors.

8. If any of the mandatory levels are missing, create them by interpolating from the existing data. If any of the mandatory levels are below the surface elevation, eliminate them from the data set.
9. Check for any missing data at the top level of the sounding. If there are missing data, make interpolations from data below or set to some reasonable value from the standard heights.
10. Truncate or round values that are not typically used in meteorological calculations. As an example, a wind speed of 23.4 kn is truncated to 23 kn.
11. There must be at least four levels in all soundings, and there must be data to at least 500 mb in the sounding.

Without these above criteria, the meteorological calculations cannot be accomplished.

3.2 Missing Data from Sounding

The ASP needs pressure, height, temperature, dew point, wind direction, and wind speed data for each level of the sounding. The TTBB data contains only pressure levels, temperature data, and dew point depression values; thus, the height of the level and the wind data are missing. The PPBB data has missing values of pressure levels, temperature data, and dew point depression data. The ASP quality control program derives these missing data.

3.2.1 Missing Temperature, Dew Point, and Wind Data

It is assumed that the atmosphere is logarithmic in pressure from the surface to the top of the atmosphere (100 mb in this case). To find any missing values of temperature and dew point, a simple linear interpolation is used. As an example, if the temperature is missing from the i^{th} level, the equation below is used to find the missing value.

$$temp(i) = temp(i-1) + [temp(i+1) - temp(i-1)] * \left\{ \frac{\log [pp(i-1)] - \log [pp(i)]}{\log [pp(i-1)] - \log [pp(i+1)]} \right\} \quad (1)$$

To interpolate the wind direction data, it is necessary to

- convert these data into u and v components of the wind,
- interpolate the values using Eq. (1), and
- convert back from the u and v components to the wind direction in degrees.

3.2.2 Missing Height Data

In the case of the TTBB data, the height values at the i^{th} level are missing. To find the missing height value, the hypsometric equation is used:

$$height[i] = elev + 287.04 * \frac{(\bar{T}_v + 273.16)}{(9.806)} * \log \left[\frac{pp(sfc)}{pp(i)} \right] \quad (2)$$

where

- | | | |
|-------------------------|---|--|
| elev | = | the height of the elevation in meters |
| 287.04 | = | the value of the gas constant for dry air |
| \bar{T}_v | = | the mean virtual temperature in degrees C |
| 273.16 | = | the value added for degrees Kelvin |
| 9.806 ms^{-2} | = | the gravitational acceleration |
| pp | = | the pressure values for the surface and the missing level, i |

3.2.3 Missing Pressure Data

In the PPBB data, only the height and wind data are delivered. Since these data are useful in the ASP, it is necessary to calculate the pressure values missing in the PPBB data or for any level in which pressure is missing. Equation (3) calculates the missing pressure level (i).

$$Pvalue = \log [pp(i+1)] + \frac{[ht(i+1) - ht(i)]}{[ht(i+1) - ht(i-1)]} * \{\log [pp(i-1)] - \log [pp(i+1)]\} \quad (3)$$

where

- i-1 level = the pressure level below the one missing
- i+1 level = pressure level above the one missing
- ith level = the height for the missing pressure level

In order to find the missing pressure level, the value is raised exponentially, and the missing pressure is derived. These missing levels are placed into the ASP sounding.

3.3 Quality Control of the BFM Output Data

Once the BFM data is accessed for a grid cell at its center point, the ASP eliminates the surface-derived data or first level. Since surface temperature and moisture observations are normally recorded at 2 m above ground level (AGL), the ASP accepts the 2-m level as the surface level temperature and dew point. The surface wind is considered to be 10 m AGL. This eliminates many problems that would occur if the BFM zero-level data were used. The wind data at ground level is set to zero by the model and the model's 10-m level is used as surface wind.

There is no other quality control of BFM data since the BFM program has its own quality control program. For details about the BFM quality control program see Henmi and Dumais. [5]

4. Stability Analysis from the Sounding Data

After the quality control program is completed, these data from the atmospheric sounding or from the mesoscale model are processed. These data are placed into six arrays:

- pressure
- height
- temperature
- dew point
- wind direction
- wind speed.

From these data it is possible to derive many products that are useful for forecasters. These calculations include a large set of thermodynamic variables and levels that furnish information about the stability of the atmosphere.

4.1 Thermodynamic Variables

Stability analysis of the atmosphere is an essential element in convective forecasting. Since stability analysis is a complex and time-consuming process, a number of convective indices have been developed to simplify this task. This section describes information on the calculation of both stability indices and thermodynamic levels in the ASP. [6]

4.1.1 Vapor Pressure Calculation

This calculation uses a formula by Tetens:

$$e_s = 6.11 * 10^{\left(\frac{a*t}{b+t}\right)} \quad (4)$$

where e_s is saturation vapor pressure, t is temperature in degrees Celsius, and constants a and b = following values:

$$\begin{array}{ll} \text{over water } a & = 7.5, & b = 237.3 \\ \text{over ice } a & = 9.5, & b = 265.5 \end{array}$$

4.1.2 Relative Humidity

The mixing ratio is defined by:

$$w = \frac{0.622 * e}{p - e} \quad (5)$$

where w is the mixing ratio, p is the ambient air pressure, e is the partial pressure due to the water vapor. Use the subscript s on e to denote saturation mixing ratio.

To calculate the surface relative humidity (RH), use Eq. (6).

$$RH = 100 * \frac{W}{W_s} \quad (6)$$

where the surface RH is the ratio of the mixing ratio to the saturation-mixing ratio multiplied by 100 percent.

4.1.3 Convective Condensation Level

The convective condensation level (CCL) is the point of intersection of the temperature curve on the skew $T - \log P$ diagram with the saturation mixing ratio line corresponding to the average mixing ratio in the surface layer.

[7]

The CCL is found graphically as the point of intersection of the mean mixing ratio with the temperature curve on the sounding. The mean mixing ratio is calculated in the lowest 100 mb on the sounding. To find the point of intersection, use the following linear interpolation:

$$PCCL = \frac{W_s(i-1) - W(avg)}{W_s(i-1) - W_s(i)} * [pp(i) + pp(i-1)] \quad (7)$$

where

PCCL = the pressure level of the CCL
W = the mixing ratio
W_s = the saturation mixing ratio
pp = the pressure level
i = the higher level
i-1 = the lower level

The convective temperature is then found by bringing a parcel dry-adiabatically from the CCL back down to the surface pressure. Poisson's equation is used to perform this calculation and is given by:

$$ConvT = T_{ccl} \left(\frac{P_{sfc}}{P_{ccl}} \right)^{\frac{R}{C_p}} \quad (8)$$

where

ConvT = the convective temperature in degrees Kelvin
T_{ccl} = the temperature in degrees Kelvin at the CCL
P_{sfc} = the surface pressure in millibars
P_{ccl} = the pressure in millibars at the CCL
R = the dry air gas constant
C_p = the specific heat of air at constant pressure

4.1.4 The Lifted Condensation Level

The lifted condensation level (LCL) is the level to which a parcel of moist air must be lifted adiabatically before it becomes saturated with respect to water.

To find the height of the LCL, first compute the mean temperature between the initial level of the parcel and the LCL (based on pressure), then use the formula

$$HTLCL = 287.04 * \frac{\bar{T}}{9.806} * \log(P_o / PLCL) \quad (9)$$

where

- HTLCL = the height of the LCL
- \bar{T} = the mean temperature of the layer in degrees Kelvin
- P_o = the surface pressure
- PLCL = the pressure level of the LCL

4.1.5 Other Thermodynamic Variables

The level of free convection (LFC) is found at the height at which a parcel of air lifted dry-adiabatically until saturated and saturation-adiabatically thereafter would become warmer (less dense) than the surrounding air. The equilibrium level (EL) is the level in the atmosphere where a rising parcel of air reaches a stable layer and no longer can rise above this layer. The EL is based on the temperature and pressure of the LCL. Thus, the less stable the conditions at the level of the LCL, the higher will be the EL. [7]

The freezing level is referred to the lowest level in the atmosphere at which air temperature 0°C is reached. In some cases, the freezing level can be obtained in more than one instance such as a case where an inversion layer is present.

The tropopause is the boundary between the troposphere and stratosphere. It is associated with a rapid change in the temperature and moisture curves on a skew T - log P.

4.2 Calculation of Stability Indices

To calculate many of the conventional stability indices, the following parameters must be known at three mandatory levels.

1. 850 mb temp, dew point, wind speed, wind direction
2. 700 mb temp, dew point
3. 500 mb temp, wind speed, wind direction

If data are not available at these mandatory levels, as will be the case with BFM output, an interpolation scheme computes values for the missing levels. Additionally, many of these stability indices cannot be calculated at locations where the surface pressure is less than 850 mb, or they may be exaggerated at locations where the surface pressure is just above 850 mb.

4.2.1 *K Index*

The K index is a useful parameter for forecasting general nonsevere (air-mass thunderstorms) convection. Usually, when the K index exceeds 30, the atmosphere is warm and moist in the lower levels and relatively cool at 500 mb. The K index is sensitive to the dew point depression at 700 mb and obtains a lower value when the relative humidity is low at 700 mb.

This can account for the effects of entrainment of dry air into the thunderstorm environment, a condition that is regarded to be favorable for the development of severe thunderstorms. The K index is calculated as follows:

$$K = T_{850} - T_{500} + TD_{850} - (T_{700} - TD_{700}) \quad (10)$$

The total totals are a combination of the cross totals and vertical totals.

where

$$\text{vertical totals} = T_{850} - T_{500}$$

$$\text{cross totals} = TD_{850} - T_{500}$$

$$\text{total totals} = \text{vertical totals} + \text{cross totals}$$

The cross totals reveal the relationship between low-level moisture and the temperature at 500 mb. Typically, cross totals in excess of 18 are considered necessary for convection.

The vertical totals are similar to the cross totals except the 850-mb air temperature is considered rather than the dew point depression. A threshold value of 26 is a threshold value for deep convection.

The total totals are a better parameter for convection than the cross totals or vertical totals alone. A threshold value for the development of thunderstorms is 44.

4.2.2 Showalter Index

The Showalter index is a measure of the local static stability of the atmosphere. This index is determined by raising an air parcel from the 850-mb level dry-adiabatically to the point of saturation, then saturation-adiabatically to 500 mb. At the 500-mb level, the temperature of the parcel is compared to that of the environment; the magnitude of the index is the

difference between the two temperatures. If the parcel is colder than its new environment, the index is positive; if it warmer, the index is negative. [7]

4.2.3 *Lifted Index*

The lifted index (LI) is calculated by using the mean temperature and mixing ratio for the lowest 100 mb of the sounding, then lifting the mean temperature and dew point from 50 mb above the surface. The LI compares the low-level heat and moisture with the 500-mb temperature. It gives a measure of buoyancy that a boundary-layer parcel would have if it ascended moist adiabatically after reaching the LCL. Generally, an LI of 0 or less is an indicator that convection is likely.

A variety of the LI is the surface lifted index (SLI). It uses the surface temperature and mixing ratio and lifts from there.

4.2.4 *Threat Index (SWEAT)*

The severe weather threat index (SWEAT) was calculated by Miller. [8] It is calculated in Eq. (11):

$$SWEAT = 12 * TD_{850} + 20 * (Totals - 49) + 2 * FF_{850} + FF_{500} + 125(S + 0.2) \quad (11)$$

where Totals refers to the total totals index and S is Sin (500 mb to 850 mb wind direction) and wind direction is in degrees.

The last term, the shear term, $125(S + 0.2)$ is set to zero if any of the following conditions are not met:

- 850 mb wind direction in the range 130° through 250° ,
- 500 mb wind direction in the range 210° through 310° ,
- 500 mb wind direction minus 850 mb wind direction positive, and
- both the 850 and 500-mb wind speeds are at least 15 kn.

No term in the formula may be negative. [8]

The first term in the SWEAT index suggests that adequate low-level moisture is necessary. The second term gets large as total totals increases. The final three terms in the equation quantify the importance of strong low- and mid-level winds and the directional shear between them. The threshold for severe thunderstorms is a SWEAT index value greater than 300, and the threshold for tornadoes is a value of 400.

More recently, Moncrieff and Green developed a parameter that measures the convective available potential energy (CAPE). CAPE is defined in Eq. (12):

$$CAPE = \int_{CCL}^{EL} g(\theta_p - \theta_{env}) * dz \quad (12)$$

where

- g = the gravitational acceleration
- θ_p = the potential temperature of the parcel
- θ_{env} = the potential temperature of the environment
- dz = difference in height between two levels of the sounding

By definition, CAPE is found by integrating from the level of the CCL to the level of the EL. Thus, it is the difference between the potential temperature of the environment and the potential temperature of the parcel at each pressure level given in the sounding between the CCL and EL. [9, 10]

The Bulk Richardson number (BRN) is useful because it helps the forecaster determine what type of storm may develop in a given environment. The BRN is defined in Eq. (13):

$$BRN = \frac{PBE}{1/2 \times U^2} \quad (13)$$

The PBE is the potential buoyant energy for a lifted parcel in the storm's environment and is calculated nearly the same as the CAPE, except for each vertical step, the equation is divided by the potential temperature of the environment. U is the measure of the vertical wind shear through a relatively deep layer (0-6 km AGL). U is calculated by deriving the difference between the mean wind over the lowest 6 km of a profile and a surface layer wind (500-m mean wind). The calculation for U is shown below:

$$\overline{U} = \overline{U}_{6000} - \overline{U}_{500} \quad (14)$$

Results from Weisman and Klemp have shown that, supercell formation is generally confined to values of BRN between 10 and 40. [11,12]

4.2.5 *Boyden, S, and Ko Indices*

Three stability indices typically used in Europe are included in the ASP. The Boyden index measures the thickness of the layer from 700 to 1000 mb and divides this value by 10. The 700-mb temperature is in degrees Celsius. The calculation is then completed as shown in Eq. (15):

$$Boyden = 700 \text{ mb Temp} + \text{thickness} - 200 \quad (15)$$

The S-index uses a variable to show the influence of the vertical totals. If the vertical totals ≥ 25 , then $\text{var}=0$. If $22 < \text{VT} < 25$, then $\text{var}=2$. If the vertical totals is ≤ 22 , then $\text{var}=6$. The equation for S-index is show below:

$$S\text{-index} = \text{Total Totals} - (700 \text{ mb Temp} - 700 \text{ mb dew point}) - \text{Var} \quad (16)$$

where temperature and dew point are in degrees Celsius.

The Ko index is the final European index used. It measures the difference in potential temperature from the mid- to low-levels. In the ASP, the mid-levels were considered 600 mb, because there may be no BFM output at 500 mb, which is typically considered the mid-level. The low-level potential temperature was taken as 50 mb AGL. Eq. (17) displays the Ko index.

$$Ko = \theta_{600 \text{ mb}} - \theta_{\text{low}} \quad (17)$$

4.3 Precipitable Water

The precipitable water is the total atmospheric water vapor contained in a vertical column extending between two specified levels. The total precipitable water is that contained in a column from the earth's surface to the "top" of the atmosphere. In the ASP, the top of the atmosphere is considered to be 300 mb. However, since the BFM only extends vertically to 7000 m from the highest point on a grid, often the integration is below 300 mb and can be as low at 450 mb. Mathematically, if $x(p)$ is the mixing ratio at pressure level p , then the precipitable water vapor W contained between two pressure levels is expressed in Eq. (18). [7]

$$W = \frac{1}{g} \int_{p_1}^{p_2} x dp \quad (18)$$

5. Weather Hazards

While analysis of skew T - log P diagrams supply useful information about the stability of the atmosphere, there is a need for much more detailed weather output. After completion of the BFM run, data are placed into the GMDB. These data include model output of temperature, moisture, wind vector components, and pressure levels. Such data are helpful for Army operations. However, using the above variables (temperature, moisture, wind components), derived parameters such as ceiling height, turbulence, icing, thunderstorm probability, severe weather, and surface visibility provide supplementary information for Army applications.

Battlefield systems are impacted by the weather. Today's weapons and sensors may be even more sensitive to weather than in the past. High technology weapon systems such as the advanced tactical missile system and the Apache helicopters can be degraded, as can be many of the intelligence collection systems. The goal of the weather hazards program is to optimize weapon performance, assist in troop maneuvers, and aid the staff weather officer with weather guidance. [13]

The hazards program provides automated analysis and forecasts of what are considered "hazards" to Army operations. Additionally, the Integrated Weather Effects Decision Aid (IWEDA) program uses many of the derived parameters in the ASP program. The IWEDA uses the ASP and BFM output to provide detailed information in terms of why, when, and how weather affects weapon systems (as well as their subsystems and components) and operations. [14]

Often in weather forecasting, decisions must be made instantaneously; thus, it becomes beneficial to implement artificial intelligence (AI) techniques to assist in weather forecasting. However, the weather hazards program is not true AI, because it uses statistical data, conventional computer programming techniques, and basic meteorological calculations as a first "guess" at the hazards. It becomes advantageous to use IF-THEN rules to assist in making

weather products such as turbulence and clouds. The hazards program makes an initial prediction and then gains information as it advances through the software in a top-down or forward-training methodology. This is called a heterogeneous expert system, because there is an integration of existing software with a rule-based expert system. [1]

As an example, the cloud forecast is based on a continuous sequence of rules that uses relative humidity data, derived lapse rates, moisture depth, wind data, time of day, seasonal influences, and location of the station. All these facts are synthesized by a set of rules to make a forecast of cloud height, ceiling height, depth of the cloud, and cloud amounts (scattered, broken, or overcast).

As a stand-alone program, the weather hazards program derives the turbulence, icing, clouds, and inversion layers (figure 3).

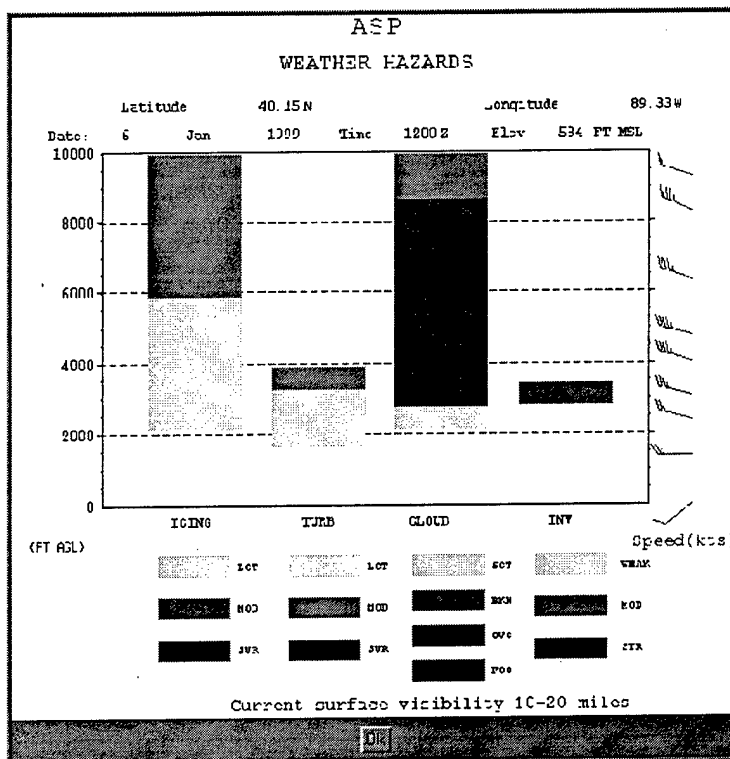


Figure 3. Plot of ASP weather hazards based on sounding observation.

5.1 Turbulence

Treating the atmosphere as a fluid, turbulence is generally a state of fluid in which there are irregular velocities and apparently random fluctuations. These oscillations in the atmosphere can adversely affect airframe performance and endanger Army aircraft. Turbulence is present in and near thunderstorms, as can be expected, based on dramatic updraft and downdraft speeds. Typically, a thunderstorm is a warning sign that turbulence will be present, and that pilots need to make adjustments to their flight plans in the vicinity of convective clouds. [7]

However, forecasting clear air turbulence (CAT) is a much more difficult problem. Rammer related synoptic patterns to the observation of CAT. Ellrod and Knapp listed several mesoscale environments where significant CAT was found to be prevalent. The study by Ellrod and Knapp associated vertical wind shear, deformation, and convergence into a single index. Work done by Lake, and more recently Black and Marroquin, have related calculations of kinetic energy to areas of forecasted turbulence. [15,16,17,18]

Theoretical studies and empirical evidence have associated CAT with Kelvin-Helmholtz instabilities. Miles and Howard indicate that the development of such instabilities require the existence of a critical Richardson number (RI) ≤ 0.25 . The RI is expressed as a ratio of the buoyancy resistance to energy available from the vertical shear. The equation is expressed below:

(19)

$$RI = \frac{\frac{g}{\theta} * \left(\frac{\partial \theta}{\partial Z} \right)}{\left(\frac{\partial V}{\partial Z} \right)^2}$$

where

g = gravitational acceleration

$\partial \theta / \partial Z$ = change of potential temperature with height

∂V = vector wind shear occurring over the vertical distance ∂Z .

[19, 21]

Once turbulent eddies have occurred in the stably stratified atmosphere, they can be maintained only as long as the work required to overcome the buoyancy resistance is less than that available from the shear of the layer.

Because the ASP uses a single one-dimensional (vertical) sounding, it was impossible to incorporate techniques such as the index developed by Ellrod and Knapp, which relies on 3-D horizontal and vertical motion fields. Early methods employed in this study to analyze or forecast turbulence included empirical methods (wind speed) and a vertical-shear method. Both of these methods displayed little skill, as might be expected, since turbulence is much more complicated than looking at the effects of wind speed or wind shear alone. [16]

Of all the methods using a single sounding, the RI proved to make the most sense physically because it included the influence of both the temperature and shear in the atmosphere. Additionally, in agreement with McCann, the RI displayed the most skill of the methods tested using a single sounding. [21]

The U.S. Navy Fleet Numerical Meteorological and Oceanography Center (FNMOC) uses the Panofsky index (PI) to forecast low-level turbulence, where the low level is considered to be below 4000 ft AGL. The formula for this index is:

$$Panofsky\ index = (windspeed)^2 * (1.0 - \frac{RI}{RI_{crit}}) \quad (20)$$

where RI is the RI and RI_{crit} is a critical RI empirically found to be 10.0 for the FNMOC data. The higher the Panofsky index, the greater the intensity of turbulence at low levels.

Based on analyses of raw RAOB data and corresponding pilot reports, early results of this work (using the Panofsky index in the lower levels and the RI

above 4000 ft) show a strong bias to underforecasting turbulence. Thus, the following adjusted values were used to determine the intensity of turbulence:

For levels <4,000 ft AGL

No turbulence	PI <60.0
Light turbulence	PI 60-100
Moderate turbulence	PI = 100-250
Severe/Extreme turbulence	PI >= 250

For the RI, adjustments were also made due to the bias of underforecasting turbulence.

For levels >4,000 ft AGL

No turbulence	RI >1.00
Light turbulence	RI 0.25-1.00
Moderate turbulence	RI 0.12-0.25
Severe/Extreme turbulence	RI <0.12

While this combination of the RI and the PI was useful to predict turbulence, some additional rule-checks were developed to ascertain that the derived numerical values made physical sense.

As an example, there are checks for each level of the sounding or model output. The program checks the wind velocities and temperature values against the "forecast" for turbulence. If there is a forecast for severe turbulence in a case where wind speeds are <25 kn, there is no shear present in the layer, and the temperature gradient is small, then the turbulence is reduced from severe to light to correspond with what is most commonly observed by pilots under these circumstances. While these errors are rare, these useful checks help increase the accuracy of the turbulence analyses and forecasts.

There are methods of turbulence generation other than wind speed, wind shear, and unstable atmospheric layers. These can include thermals and mountain waves. While it is difficult to forecast turbulence at the small scale on which it occurs, it is even more challenging with a single sounding to make forecasts for mountain waves. Thus, at the current time, no effort is made here to do so. However, a simple set of rules is used to forecast thermal instability where thermal instability is instability in a fluid caused by heating at a boundary.

5.2 Icing

One of the most vital hazards forecast is aircraft icing not associated with convection. Generally, icing occurs at temperatures between 0 and -40°C. Schultz and Politovich note that the accretion of ice on aircraft surfaces is controlled by two processes: [22]

- impaction of supercooled cloud droplets on the aircraft and
- the freezing of these droplets onto the airframe.

As may be expected, the two essential factors in forecasting icing are the temperature of the atmosphere and the availability of moisture. However, other less obvious factors such as the wind velocity, drop size, concentration of the droplets, stability of the layer, and nonmeteorological factors such as aircraft forward speed and aircraft configuration influence the icing type and intensity.

In the ASP, three types of icing are considered.

1. Rime icing is the most common type reported and according to Cornell, et al., rime icing occurs at cold temperatures and is the result of the instantaneous freezing of small supercooled droplets as they strike the aircraft.

2. Clear icing usually occurs at temperatures just below freezing and it is clear because of the slow freezing of larger supercooled liquid water droplets that are able to spread out upon impact.
3. Mixed icing occurs at intermediate temperatures and is a combination of clear and rime icing. [23]

Additionally, there are four icing intensities in the ASP.

1. Trace icing is when the icing becomes noticeable on the aircraft.
2. Light icing is when the accumulation of ice generates a problem for flights in excess of 1 h.
3. Moderate icing is when the rate of accumulation presents a problem for short flights.
4. Severe icing is when the rate of accumulation is so intense that de-icing equipment fails to repress it.

Given the restraints of the single upper-air sounding as the data source, it was determined that the best approach to the analysis/forecasting of icing was to utilize the RAOB icing tool developed at the AFWA in 1980 (formerly, the Air Force Global Weather Center [AFGWC]). The RAOB technique uses the temperature, dew-point depression, and temperature lapse rate as a measure of instability of the layer. A study by Knapp showed that the RAOB icing tool performed with the most accuracy, compared to other icing models, at all levels of the atmosphere. [24,25]

The RAOB tool is essentially a "decision tree," in that it classifies icing by temperature, dew-point depression, and lapse rate. There are three main temperature groups that are based on the theory of ice formation:

- The first case, -35 to -16°C, results in light rime icing in all cases.
- The middle class, -16 to -8°C, generally accounts for the mixed and rime cases, with the intensity based on the lapse rate or stability of the layer.
- The warmest group, -8 to -1°C, is often the temperature range when clear icing is found.

However, when the layer is stable, rime ice usually occurs. Clear ice most commonly occurs in layers of the atmosphere that are unstable and undergoing lifting.

A final case is added to account for severe clear icing. This situation occurs when there is a strong inversion about 100 mb above the surface; thus the precipitation falls from a liquid state into a sudden layer of sub-freezing temperatures. This rapid change in temperature causes the relatively warm water droplets to spread quickly on the aircraft and cause clear icing to form.

A modification that has been applied in the ASP as compared to the original RAOB tool is an allowance for higher dew point depressions since the original RAOB tool was found to underforecast icing. Cornell's study showed that the RAOB tool dew-point depressions were too stringent. This investigation of soundings showed that the mean dew-point depression for all icing types was 4.5°. This modification was made for the RAOB icing chart. [23]

5.3 Clouds

Forecasting cloud amounts, cloud heights, and cloud depth is essential for military operations. Clouds can degrade the effectiveness of many weapon systems by limiting flight paths, visibility, and making it impossible to identify targets and aircraft. A staff weather officer needs a detailed and accurate cloud forecast because of the overall influence of the weather. Clouds act to alter temperature, moisture, and wind fields at all times of the day.

Cloud drops form in the atmosphere in response to moist air becoming saturated or slightly supersaturated. In clouds, relative humidity rarely exceeds 102 percent (supersaturation of 2 percent) and is rarely lower than 98 percent. Normally, it takes dynamic lifting or atmospheric cooling to create conditions where supersaturation and related droplet growth can occur freely in the atmosphere. [26]

Unfortunately, accurate measurements of the moisture in the atmosphere are difficult. Typically, Vaisala high-performance radiosondes are used to measure the vertical moisture profile. These sondes use the carbon humidity element, which is a slender coating of fibrous material on a glass or plastic substrate. At high humidity the element swells and the carbon granules are less densely packed, resulting in an increase in resistance. The reaction of the film is rapid, but the substrate response is delayed. Because the measured humidity is with respect to the temperature of the film and the temperature is locked to the substrate, assuming air temperature and substrate temperature are the same results in errors. These errors may be as much as 10 percent in humidity, which is a significant error at high humidities. Blackmore explains that the sondes have the most difficulty measuring relative humidity in very moist situations and very dry situations. [27,28]

5.3.1 Ceilings and Relative Humidity Study

A ceiling is the height at which the sky becomes broken or overcast. Much of the emphasis in this cloud study is placed on correctly analyzing and forecasting the ceiling height.

Many methods have been used to forecast clouds. Numerical models often contain cloud physics packages and cumulus convection routines that numerically solve for cloud heights, amounts, and ceilings. Statistical methods, such as multiple discriminant analysis and the perfect prognostic method are often used in cloud forecasting. Others have experimented with neural network and AI techniques to "train" or develop a set of rules that

resolve a problem. These AI methods are easy to use, computationally stable, and consistent in their results.

The use of a neural net was not feasible in this study, because the ASP is an automated program designed to be operated at any location in the world. Thus, it would be impossible to train the neural net to work in all locations. Since the BFM is designed to run as quickly as possible, there is no current effort to forecast cumulus clouds with a cloud physics package. Using the cloud liquid water output from the BFM does not take into consideration all conditions that may influence cloud formation and cloud heights. While the cloud liquid water data is helpful in displaying water content in the atmosphere, it is not useful in correlation to clouds. A cloud liquid water value of 0.1 gm/m^2 can result in two different cloud outcomes based on temperature and location.

It was decided to approach the cloud forecasting problem with a cross between empirical techniques, statistical data, and rule-based IF-THEN sets of code. This technique was best for using the single upper-air observation in the ASP.

A statistical study was completed to contrast the soundings with observed cloud amounts and heights at National Weather Service offices around the United States. This investigation compared the ceiling height to the relative humidity value observed on an upper-air observation at 1200 UTC and 0000 UTC. The study was done with respect to season, time of day, and for a small sample, the location of the sounding.

5.3.2 Relative Humidity Values

Table 1 shows the average relative humidity values for the four ceiling groups as compared to each season. Sample sizes varied from 58 soundings during the spring months to 110 soundings during the summer months. The results show little variation in the relative humidity values "needed" to form a ceiling. Note that cloud formation is not dependent on relative humidity values alone,

but it does play a significant role. The values decrease somewhat with height, perhaps because measurement of water vapor becomes slightly less accurate with height.

Table 1. Average relative humidity values* (different seasons)

Height of ceiling (ft AGL)/season	Spring (percent)	Summer (percent)	Autumn (percent)	Winter (percent)	All seasons
<4000	96	95	93	95	95
4000-8000	95	91	94	96	94
8000-20000	93	91	90	90	91
20000+	61	56	61	67	59

***Values calculated from 1200 UTC and 0000 UTC soundings for different observed ceiling heights during different seasons.**

Due to changing observation requirements and measuring systems, ceilings are rarely reported above 12000 ft AGL; thus, the sample size of data for these layers is vastly reduced. The most vivid trend in these data is the vastly reduced relative humidity needed to form a ceiling at the cirrus level, or above 20,000 ft AGL. This is a predictable result, considering the difficulties in measuring the moisture values at higher levels and that the nucleation and formation of clouds is occurring in a layer with few supercooled water droplets and predominately ice crystals. Even here, however, there is consistency, with the values ranging from 56 to 67 percent during the year.

While it may appear that small differences in relative humidities are not consequential, work done by Walcek indicated that a 2 to 3 percent increase of the relative humidity could lead to a 15 percent increase in cloud cover. He also noticed, as in this study, that middle-level ceilings formed in lower humidity. Thus, the trends in the above chart are employed to derive the "decision tree" or flow chart that is used to form the IF-THEN rules in the cloud program. [29]

Table 2 indicates that there are only small differences in the relative humidity values that are needed to form a ceiling at different times of the day. Initially,

in this project there were different rules based on the time of day. However, the data in table 2 indicated that neither relative humidity nor moisture were factors in ceiling height, based on the time of day. This study simplified the IF-THEN rules.

**Table 2. Average relative humidity values*
(ceiling heights)**

Height of ceiling (ft AGL)	0000 UTC (percent)	1200 UTC (percent)
<4,000	94	95
4,000–8,000	93	94
8,000–20,000	91	91
20,000+	58	60

***Values calculated from 1200 UTC and
0000 UTC soundings for different observed
ceiling heights.**

Another research effort was based on the location of sounding observations. In very moist tropical locations, clouds rarely were observed despite relative humidity values of 100 percent. This trend was noticeable along the Gulf Coast of the United States on warm, humid summer mornings. Meanwhile, at many inland locations low clouds were still observed at corresponding high relative humidity values.

Cloud studies by Pruppacher show that in air-over-land, only a small fraction of the available aerosols are capable of becoming cloud condensation nuclei (CCN). However, over the oceans, the number of aerosols is reduced but larger, and more water-soluble nuclei have been observed.

There is a general trend over land for smaller hygroscopic drops, thus freeing more available water for each CCN. Over the water, the larger CCN absorb much of the free water, thus leaving very little to be lifted and condensed. Another possible theory to explain this trend may be as simple as the relatively flat terrain, or the lack of any lifting mechanism in the more tropical locations. While it is difficult to explain precisely the cause of this observation (lack of clouds at 100 percent relative humidity [RH] in warm season), it was a very worthwhile observation in the development of the ASP rules. [26]

Based on these results, it was determined to treat tropical and mid-latitude ceiling predictions as two different locations in the rules or flow chart. Thus, the two most definitive forecasting parameters for clouds were found to be the site location and the relative humidity value of the layer with respect to height in the sounding.

Mesoscale models often display a dry bias. Schultz observes that relative humidity values in excess of 55 percent between 500 to 1000 mb usually identify regions with widespread cloudiness on the Nested Grid Model. The BFM does not display such an extreme bias; however, clouds are often observed in layers with relative humidity well below values of saturation. [22]

A study using 13 runs of the BFM was done to investigate the differences between the BFM output and observed soundings. This study, using model runs in various regions of the United States, over different seasons, shows that relative humidity differences with model output increase with height and time from the initialization of the model.

Table 3 displays what might be expected: a drier model output in comparison to measured relative humidity by the soundings. The model moisture is fairly consistent at all levels at the initial time; however, the model is 5 to 10 percent drier at the 12-h and 24-h periods. These data indicate that making cloud predictions from the BFM model output would require a definite reduction in the relative humidity values, with the greatest differences occurring at lower pressure levels and with increasing time.

Table 3. Difference in BFM output*

Pressure levels/Time from initialization	00-h forecast	12-h forecast	24-h forecast
925 mb	3% drier	5% drier	11% drier
850 mb	3% drier	8% drier	9% drier
700 mb	2% drier	10% drier	11% drier
500 mb	3% drier	3% moister	12% drier

***Difference in the BFM against the observed sounding, based on hours from initial time and different pressure levels.**

The one deviation in this trend, the 12-h forecast at 500 mb, cannot easily be explained. At the initial hour, 53 to 63 percent of the model runs were drier than the observed soundings. At the 12-h forecast period, the model was drier than the soundings 65 percent of the time; and finally, at 24 h the model was drier 71 percent of the time.

Another trend in this cloud study was the lack of any low clouds in the tropical locations during the summer season. A study of Northern Hemisphere tropical observations at 1200 UTC (73 samples) indicated no cases of scattered clouds below 1,000 ft AGL. Scattered clouds below 2,000 ft AGL were observed in only 7 percent of the cases. Only 5 percent of all tropical soundings reported a ceiling below 4,000-ft AGL (summer season). At 0000 UTC, the results were only slightly different. Using a sample of 39 tropical observations, in only 10 percent of the cases was there a ceiling below 4,000 ft AGL, and only 3 percent had scattered low clouds observed below 1,000 ft AGL. This study displayed that low scattered clouds were infrequent in the tropics and are eliminated from the rule set during the warm season.

A final observation in this study indicated that cumulus cloud formation was being underforecasted. This led to the development of an empirical check for cumulus clouds. In this empirical check, during the time of maximum heating (1100–2000 local), cumulus clouds were formed if the convective temperature was being approached or exceeded. The calculation for the convective

temperature is discussed in section 4.1.3 of this report. There is no effort to show the vertical development of the cumulus cloud; thus, it cannot be assumed that a thunderstorm will form from this cloud layer.

A final set of checks in the cloud program are listed below:

1. No clouds were allowed above 30,000 ft AGL.
2. Since all high relative humidity values below 200 ft AGL were being interpreted as a cloud, no clouds were analyzed or forecasted under 200 ft AGL. These high humidities are often seen as fog and not clouds on the output.
3. A check was made to examine the depth of a moist layer. Small moist layers were being labeled as cloud layers, yet were rarely observed to be clouds. Thus, these shallow, elevated moist layers were not listed as clouds in the program.

5.4 Thunderstorms

Forecasting thunderstorms is an important element in weather hazards forecasting. Other than the understandable influences of turbulence on Army aircraft, thunderstorms also bring heavy rain, lightning, and sometimes severe weather such as hail, damaging wind, and tornadoes. All these weather phenomena can hamper communications and maneuverability and can cause damage to sensitive equipment.

From a forecasting perspective, thunderstorms can radically change the local temperature and moisture content in a matter of minutes. Additionally, cloud cover from these convective storms can spread miles away and cause changes to the weather conditions far away from the storm itself.

5.4.1 Thunderstorm Probability

The automated thunderstorm program was developed for a single-station location using a 0000 or 1200 UTC upper-air observations. This provided a 12-hr forecast of a "yes/no" forecast of thunderstorms and later a probability of thunderstorms was implemented into the program. The original method of the program was to use an expert system shell called EXSYS. Weather parameters such as the values of the stability indices were input into the expert shell, and a decision was reached as information processed through the expert system.

Later, the "C" Language Production System (CLIPS) programming language was utilized in an effort to give the forecaster some interaction with the system. In addition to the stability parameters, the user was able to add information about the atmospheric dynamics or "lifting" mechanisms that might help thunderstorm initiation.

While these expert system approaches were very functional and granted excellent skill scores, rapid changes in Army computer platforms and frequent changes in software languages made it impossible to use these expert systems. It was determined that the most efficient and dependable method to forecast thunderstorms was to formulate an equation using statistical methods.

The equation was derived with the goal of accurately predicting percent probabilities of local thunderstorm occurrence within a 100-km radius of a RAOB location. Data from 1200 UTC soundings at 13 different climatological locations across the continental United States were collected from March to October of 1990 and 1993. Testing a variety of stability indices, these data were verified by thunderstorm reports from surface observations, National Weather Service radar summaries, and output from the National Lightning Detection Network. [30]

Multivariate discriminate analysis, using stepwise procedures, was employed to calculate the most significant thunderstorm predictors. This statistical

method created the list of thunderstorm predictors (stability indices) correctly grouped to find the combination with the highest correlation coefficient with statistical significance (using the F-test). The predictand, or thunderstorm occurrence/nonoccurrence during the 12 h after RAOB time, was given a value of "1" (yes) for any verification of thunderstorms within a 100 km radius of the station and a "0" for no thunderstorms. These "yes/no" values were correlated with the predictor indices to determine a percent probability regression equation. The discriminate analysis procedure eliminated all but three indices as the predictands: K, LI, and SWEAT. The resulting equation was:

$$\text{Percent Probability} = [0.1795 + 0.0073(K) - 0.0149(LI) + 0.0008(SWEAT)] \times 100 \quad (21)$$

where K is the K-index, LI is the lifted index, and SWEAT is the SWEAT index.

Since stability indices such as the K index and the SWEAT index cannot be computed for high-elevation stations with surface pressure less than 850 mb, a second equation was formulated from possible stability parameters at such elevations. The statistical method described above was used, and the resulting equation for high-elevation locations was:

$$\text{Percent Probability} = \{1.1806 - [0.0339 * (LI + 20.0)]\} \quad (22)$$

The probability determined by the equations does not alone answer the question about thunderstorm probability. The value added from such factors as solar radiation, time of day, dynamical lifting, moisture content, depth of the moist layer, capping inversions, season, and statistical bias is built into the system. As an example, the sounding at 1200 UTC can change dramatically during a 12-h forecast period. A station with a shallow moisture profile may mix out the moisture very rapidly, thus the program checks to see whether the moisture is shallow; if so, the probability of thunderstorms will be reduced. While it is impossible to cover all meteorological factors that contribute to thunderstorm formation, the regression equations and consequential rules add

information that provides useful guidance in forecasting thunderstorm probability.

5.4.2 Thunderstorm Severity

Severe thunderstorms are much more difficult to forecast than nonsevere convection. Severe thunderstorms are thunderstorms in which wind gusts over 50 kn are recorded, hail $>3/4$ in. diameter is observed, or where tornadoes occur. While these thunderstorms are rare compared to the total number of annual thunderstorms, they can produce a significant amount of damage.

Severe thunderstorms occur in different environments based on moisture and elevation. Generally, in moist environments, thunderstorms will have more intense rainfall amounts and will have higher precipitable water. In higher elevations, the value of precipitable water is often lower and severe thunderstorms feature hail and gusty surface winds caused by evaporative cooling (or downbursts) from the storm.

The severe thunderstorm routine is divided into four cases: moist and low-elevation storms, moist and high-elevation storms, dry and low-elevation storms, and dry and high-elevation storms. Some of the variables checked, using data from the sounding, are the mid-level moisture values, low-level jet, 500 mb (mid-level) wind speed, SWEAT index, CAPE, temperatures of the sounding, and the LI.

Once the routine determines if a severe thunderstorm is likely, an additional "rule" is used to determine what type of severe weather is likely: tornadoes, hail, or damaging winds.

5.4.2.1 Thunderstorm Gusts

Modern improvements in Doppler radar enable the forecaster to see, with great confidence, strong winds in the environment of a thunderstorm. However, it does not provide several hours of advance warning as is necessary

for military operations. While it is difficult to forecast the exact intensity and location of microburst and thunderstorm outflow, it is feasible to find favorable environments of such conditions using an upper-air observation.

Three empirical equations are combined to form an average wind-gust value. The first equation uses the difference between the wetbulb potential temperature layer and the surface. This method is based mainly on the temperature variation from the surface to the wetbulb level in the sounding. Two other methods are described by Novlan, who discusses a method from Fawbush and Miller that uses the difference between the temperature intersection of the moist adiabat and the free temperature at the 600-mb level. The second method was developed at NASA and uses the difference between the convective temperature and wetbulb zero level. These three methods are averaged to provide a "consensus" value of peak thunderstorm gust. [31]

McCann explains that microbursts develop as a result of frozen precipitation falling through the melting level. Latent heat due to melting cools the air parcels, and they become negatively buoyant and accelerate downward. Evaporation continues the process. McCann discusses the "Wind INDEX" or WINDEX method, which was implemented into the ASP as a second index for forecasting microbursts. WINDEX is essentially an empirical value based on the height of the mixing ratio, low-level moisture, and the lapse rate of the sounding from the surface to the melting level. [32]

McCann's WINDEX equation is:

$$WINDEX = 5 * [H_M * R_Q (\Gamma^2 - 30 + Q_L - 2Q_M)]^{0.5} \quad (23)$$

where

- H_M = height of the melting level above the ground,
- R_Q = $Q_L/12$ but is not greater than 1,
- Γ = lapse rate from the surface to the melting level,
- Q_L = mixing ratio in the lowest 1 km above the surface, and
- Q_M = mixing ratio at the melting level.

The WINDEX estimates that maximum potential wind gusts at the surface in knots.

5.4.2.2 Thunderstorm Movement

The method to forecast storm speed and direction are elementary since it involves only the 700- and 500-mb wind. The mean storm speed is calculated by taking an average of the 700- and 500-mb wind speed. The forecasted direction or steering of the storm is done in a similar way, using the average direction of the 700- and 500-mb wind used.

5.5 Surface Visibility

Low visibility is another example of a weather hazard that would impact military ground and air operations. Analogous to the thunderstorm prediction, a statistical method was employed to forecast the surface visibility using a radiosonde or mesoscale model output. Knapp explains that surface data from 2790 observations were collected for 80 U.S. locations from July 1994 to April 1995. These observations represented various climatic regions in an effort to compile an "average" database for deriving the universal visibility equation. For each observation, visibility values were placed into one of eight categories ranging from <1 mi to >20 mi. [33]

To develop the regression equations, Knapp used several meteorological parameters. These included:

- station elevation,
- temperature and dew point,
- dew point depression,
- relative humidity,
- wind speed,
- ceiling height, and
- precipitation reported.

At the current time there is no effort to determine if precipitation is falling at a sounding location or a model grid point.

From the 2790 surface observations, three types of equations were formulated, which account for different conditions based on available surface observation data. These three equation types were:

1. all cases, ceiling and precipitation unknown;
2. ceiling known, precipitation unknown; and
3. ceiling and precipitation known.

Screening regression techniques using stepwise procedures were used to determine the predictor values for each equation type. Once the "best" correlated predictor was found, other predictors were then included to achieve the best statistical results.

As an example, the equation developed using observations with derived ceilings is listed below:

$$VISCAT = 8.06 + (0.0003 * ELEV) - (0.0456 * RH) + (0.0058 * CIG) \quad (24)$$

where VISCAT is the category of the predicted surface visibility, ELEV is the surface elevation, RH is the relative humidity, CIG is the height of the ceiling.

Initial efforts to derive a single equation for each observation type was unsuccessful, thus a two-step approach was used. First, the visibility categories were divided into two groups:

- VISCAT 4 and below and
- VISCAT 5 and above.

Then, an equation was tailored to each group for fine-tuning. Finally, for each equation empirical adjustments are made based on the ceiling and surface visibility. As an example, by using the above equation, the following empirical adjustments are made.

If VISCAT= 4 and CIG \geq 30 and RH $<$ 95, change VISCAT to 5.

If VISCAT= 5 and CIG \leq 10, change VISCAT to 4.

If VISCAT= 5 and Temp-Dew point $<$ 3 and 10 \leq CIG \leq 15 change VISCAT to 4.

If VISCAT \leq 4 then apply a new equation for this category.

5.6 Inversion Levels

A temperature inversion occurs when the atmospheric temperature warms with height. In the ASP, this warming must be at least $0.5^{\circ}\text{C}/\Delta Z$ to be considered strong enough to be an inversion. The value of ΔZ is variable and is the thickness of each layer—either from model output or rawinsonde data. While it is arbitrary, the strength of the inversion in the ASP is as follows:

- inversion $< 1^{\circ}\text{C}/\Delta Z$ is a weak inversion
- inversion $1\text{--}3^{\circ}\text{C}/\Delta Z$ is a moderate inversion
- inversion $> 3^{\circ}\text{C}/\Delta Z$ is a strong inversion

The height of the inversion is the point at which the atmosphere begins to warm. This height is listed in meters AGL.

6. Summary

The IMETS is an automated weather data receiving, processing, and disseminating system utilized by U.S. Air Force weather forecasters in support of U.S. Army operations. As a component of the IMETS software, the ASP calculates, interpolates, and displays meteorological data for the forecaster. The ASP ingests sounding data either from conventional radiosonde data (1200 or 0000 UTC) or from 3-D model output. Once these data have been read, the program will process and display weather products so that users can make vital decisions concerning the influence of weather on military planning.

The influence of weather hazards on tactical operations is of most concern to military leaders. These hazards include icing, turbulence, inversion layers, surface visibility, and thunderstorms. Recent efforts have centered on employing sounding data to display these weather parameters. However, with the development of an operational mesoscale model, BFM, there has been an effort to make short-term weather forecasts (≤ 24 -h) of these weather hazards.

Since the ASP is a single-station vertical scan of the atmospheric sounding data, most applications used in the program are either flow-chart type of diagrams, expert system approaches using a set of rules, or regression equations designed for general and worldwide use. Turbulence is analyzed and forecasted in the ASP by using the Panofsky index below 4000 ft AGL, and the RI above 4000 ft AGL. For icing, the RAOB tool originated at AFWA has been modified and is now used in the ASP.

Cloud forecasts were developed through careful investigation of moisture properties on skew T-log diagrams through many different weather environments. This part of the ASP is the most "rule-based" in its design and uses a series of IF-THEN rules based on relative humidity, height of level, time of the day, season, and location of the station.

The thunderstorm and visibility forecasts make use of regression equations developed to work in any general weather situation. Separate equations are

used for low elevation and mountain locations for thunderstorm probability forecasts. Both the thunderstorm and visibility routines have a set of rules used after the regression equations have output their value. These rules check certain atmospheric conditions not used in the development of the regression equations.

References

1. Passner, J. E., "Expert Systems and Empirical Rules Used for Army Operations on IMETS," *Proceedings of the 13th Conference on Weather Analysis and Forecasting*, Vienna, VA, pp. 608-611, 1993.
2. U.S. Department of Commerce, *Federal Meteorological Handbook No. 4, Second Edition, Radiosonde Code*, Washington, D.C., 1976.
3. Lee, M.E., "U.S. Army Battlescale Forecast Model Concept of Operation," *Proceedings of the 1994 Battlefield Atmospherics Conference*, White Sands Missile Range, NM, 1995.
4. Henmi, et al., *Battlescale Forecast Model and its Evaluation Using White Sands Missile Range Meteorological Data*, ARL-TR-569, U.S. Army Atmospheric Research Laboratory, White Sands Missile Range, NM, 1995.
5. Henmi T. and R. E. Dumais Jr., *Description of the Battlescale Forecast Model*, ARL-TR-1032, U.S. Army Atmospheric Research Laboratory, White Sands Missile Range, NM, 1998.
6. Doswell, et al., "Thermodynamical Analysis Procedures at the National Severe Storms Forecast Center," *9th Conference on Weather Forecasting and Analysis*, Seattle, WA, pp. 301-308, 1982.
7. American Meteorological Society, *Glossary of Meteorology Fifth Edition*, Boston, MA, 1959.
8. Miller, R. C., *Notes on Analysis and Severe-Storm Forecasting Procedures of the Air Force Global Weather Central*, Tech. Report 200 (revised), Air Weather Service, Offutt Air Force Base, NE, 1972.
9. Moncrieff, M.W., and J.S.A. Green, "The Propagation and Transfer Properties of Steady Convective Overturning in Shear," *Quart. J. Royal Met. Soc.*, **98**, pp. 336-352, 1972.
10. Johns, R. H., et al., *Some Wind and Instability Parameters Associated With Strong and Violent Tornadoes. Part II: Variations in the Combinations of Wind and Instability Parameters*, National Severe Storms Forecast Center, Kansas City, MO, 1991.

11. Weisman, M.L. and J.B. Klemp, "The Dependence of Numerically Simulated Storms on Vertical Wind Shear and Buoyancy," *Mon. Wea. Rev.*, **110**, pp. 504-520, 1982.
12. Weisman, M.L. and J.B. Klemp, "Characteristics of Isolated Convective Storms," *Mesoscale Meteorology and Forecasting*, P.S. Ray (Ed.), American Meteorological Society, Boston, MA, pp. 331-357, 1986.
13. Menoher, P.E. Jr., "Weather Support to Army Operations," *Proceedings of the 11th Annual EOSAEL/TWI Conference*, U.S. Army Atmospheric Sciences Laboratory, White Sands Missile Range, NM, pp. 3-51, 1990.
14. Sauter, David P., "The Integrated Weather Effects Decision Aid (IWEDA): Status and Future Plans," *Proceedings of the 1996 Battlespace Atmospherics Conference*, Naval Command, Control, and Ocean Surveillance Center, San Diego, CA, pp. 75-81 1996.
15. Rammer, W.A., *Model Relationship of CAT to Upper Wind Flow*, Patten National Meteorological Center Aviation Weather Forecast Branch, note, p. 14, 1973.
16. Ellrod, G.P and D. I. Knapp, "An Objective Clear-Air Turbulence Forecasting Technique: Verification and Operational Use," *Wea. Forecasting*, **7**, pp. 150-165, 1992.
17. Lake, H., "Analysis of Clear Air Turbulence," *Geophys. Res. Rep.* No. 47, Air Force Cambridge Research Center, p. 63, 1956.
18. Black, T.L., and A. Marroquin, "Preliminary Results of Turbulence Predictions for Use in Aviation Weather Forecasts," Preprint of *The Fifth International Aviation Weather Systems*, American Meteorological Society, Vienna, VA, pp. 461-462, 1993.
19. Miles, J.W. and L.N. Howard, "Notes on Heterogenous Shear Flow," *J. Fluid Mech.*, **20**, pp. 331-336, 1964.
20. Keller, J.L., "Clear Air Turbulence as a Response to Meso- and Synoptic-Scale Dynamic Processes," *Mon. Wea. Rev.*, **118**, pp. 2228-2242, 1990.

21. McCann, Donald W., "An Evaluation of Clear-Air Turbulence Indices," *Proceedings of 5th International Conference on Aviation Weather Systems*, American Meteorological Society, Vienna, VA, pp. 449-453, 1993.
22. Schultz, P. and M. K. Politovich, "Toward the Improvement of Aircraft-Icing Forecasts for the Continental United States," *Weather and Forecasting*, 7, pp. 491-500, 1992.
23. Cornell D., C. A. Donahue, and K. Chan, *A Comparison of Aircraft Icing Forecast Models*, AFCCC/TN-95/004, Air Force Combat Climatological Center, Scott Air Force Base, IL, p. 40, 1995.
24. Knapp, D I., *Verification Report: Comparison of Various Icing Analysis and Forecasting Techniques*, (unpublished), Air Force Global Weather Central, Offutt Air Force Base, NE, 1992.
25. Air Weather Service, *Forecasters Guide on Aircraft Icing*, Air Weather Service, AWS/TR-80/001, Scott Air Force Base, IL, p. 61, 1980.
26. Pruppacher, H.R., "The Microstructure of Atmospheric Clouds and Precipitation," *Clouds Their Formation, Optical Properties and Effects*, P.V. Hobbs and A. Deepak (Eds), Academic Press, New York, NY, pp. 93-186, 1981.
27. Lally, V. E., Upper Air in Situ Observing Systems, *Handbook of Applied Meteorology*, David D. Houghton (Ed.), John Wiley and Sons, New York, NY, pp. 352-360, 1985.
28. Blackmore, W. H., "Environmental Chamber Tests of NWS Radiosonde Relative Humidity Sensors," Preprint of *15th International Conference on Interactive Information and Processing System for Meteorology, Oceanography, and Hydrology*, American Meteorological Society, Dallas, TX, 1999.
29. Walcek, Chris J., "Factors Influencing Regional-scale Cloud Cover: Investigations Using Satellite-derived Cloud Cover and Standard Meteorological Observations," *Proceedings of the 4th Symposium on Global Change Studies*, American Meteorological Society, Anaheim, CA, pp. 235-236, 1993.

30. Knapp, D. I. and J. E. Passner, "Development of a Local 12-hour General Thunderstorm Forecasting Technique For Use With RAOB or Mesoscale Model Vertical Profile Data," *16th Conference on Weather Analysis and Forecasting*, Phoenix, AZ, American Meteorological Society, pp. 115-117, 1998.
31. Novlan, David J., *Weather Forecast Manual*, White Sands Missile Range, NM, 1982.
32. McCann, D. W., "WINDEX C A New Index for Forecasting Microbursts," *Proceedings of 13th Conference on Weather Analysis and Forecasting*, Vienna, VA, American Meteorological Society, pp. 482-485, 1993.
33. Knapp, D. I., "Development of a Surface Visibility Algorithm for Worldwide Use with Mesoscale Model Output," *15th Conference of Weather Analysis and Forecasting*, Norfolk, VA, American Meteorological Society, pp. 83-86, 1996.

Acronyms and Abbreviations

AFWA	Air Force Weather Agency
AFGWC	Air Force Global Weather Center
AGL	above ground level
AI	artificial intelligence
ARL	Army Research Laboratory
ASP	Atmospheric Sounding Program
AWDS	Automated Weather Distribution System
AWN	Automated Weather Network
BED	Battlefield Environment Directorate
BFM	Battlescale Forecast Model
BRN	bulk Richardson number
CAPE	convective available potential energy
CAT	clear-air turbulence
CCN	cloud condensation nuclei
CCL	convective condensation level
CLIPS	"C" language production system
EL	equilibrium level
FNMOC	The U.S. Navy Fleet Numerical Meteorological and Oceanography Center

GMDB	gridded meteorological database
HOTMAC	Higher Order Turbulence Model for Atmospheric Circulations
IWEDA	integrated weather effects decision aids
IMETS	Integrated Meteorological System
LCL	lifted condensation level
LFC	level of free convection
LI	lifted index
NOGAPS	Naval Operational Global Atmospheric Prediction System
RAOBS	radiosonde upper-air observation
RH	relative humidity
RI	Richardson number
SLI	surface lifted index
SWEAT	severe weather threat index
WINDEX	wind index
WMO	World Meteorological Society

Distribution

	Copies
NASA MARSHALL SPACE FLT CTR ATMOSPHERIC SCIENCES DIV E501 ATTN DR FICHTL HUNTSVILLE AL 35802	1
NASA SPACE FLT CTR ATMOSPHERIC SCIENCES DIV CODE ED 41 1 HUNTSVILLE AL 35812	1
US ARMY STRAT DEFNS CMND CSSD SL L ATTN DR LILLY PO BOX 1500 HUNTSVILLE AL 35807-3801	1
US ARMY MISSILE CMND AMSMI RD AC AD ATTN DR PETERSON REDSTONE ARSENAL AL 35898-5242	1
US ARMY MISSILE CMND AMSMI RD AS SS ATTN MR H F ANDERSON REDSTONE ARSENAL AL 35898-5253	1
US ARMY MISSILE CMND AMSMI RD AS SS ATTN MR B WILLIAMS REDSTONE ARSENAL AL 35898-5253	1
US ARMY MISSILE CMND AMSMI RD DE SE ATTN MR GORDON LILL JR REDSTONE ARSENAL AL 35898-5245	1
US ARMY MISSILE CMND REDSTONE SCI INFO CTR AMSMI RD CS R DOC REDSTONE ARSENAL AL 35898-5241	1
US ARMY MISSILE CMND AMSMI REDSTONE ARSENAL AL 35898-5253	1
PACIFIC MISSILE TEST CTR GEOPHYSICS DIV ATTN CODE 3250 POINT MUGU CA 93042-5000	1

NAVAL OCEAN SYST CTR CODE 54 ATTN DR RICHTER SAN DIEGO CA 52152-5000	1
METEOROLOGIST IN CHARGE KWAJALEIN MISSILE RANGE PO BOX 67 APO SAN FRANCISCO CA 96555	1
DEPT OF COMMERCE CTR MOUNTAIN ADMINISTRATION SPRRT CTR LIBRARY R 51 325 S BROADWAY BOULDER CO 80303	1
DR HANS J LIEBE NTIA ITS S 3 325 S BROADWAY BOULDER CO 80303	1
NCAR LIBRARY SERIALS NATL CTR FOR ATMOS RSCH PO BOX 3000 BOULDER CO 80307-3000	1
DEPT OF COMMERCE CTR 325 S BROADWAY BOULDER CO 80303	1
HEADQUARTERS DEPT OF ARMY DAMI POI ATTN LEE PAGE WASHINGTON DC 20310-1067	1
MIL ASST FOR ENV SCI OFC OF THE UNDERSEC OF DEFNS FOR RSCH & ENGR R&AT E LS PENTAGON ROOM 3D129 WASHINGTON DC 20301-3080	1
DEAN RMD ATTN DR GOMEZ WASHINGTON DC 20314	1
US ARMY INFANTRY ATSH CD CS OR ATTN DR E DUTOIT FT BENNING GA 30905-5090	1
AIR WEATHER SERVICE TECH LIBRARY FL4414 3 SCOTT AFB IL 62225-5458	1
USAFETAC DNE ATTN MR GLAUBER SCOTT AFB IL 62225-5008	1

HQ AFWA/DNX 106 PEACEKEEPER DR STE 2N3 OFFUTT AFB NE 68113-4039	1
PHILLIPS LABORATORY PL LYP ATTN MR CHISHOLM HANSCOM AFB MA 01731-5000	1
ATMOSPHERIC SCI DIV GEOPHYISCS DIRCTRT PHILLIPS LABORATORY HANSCOM AFB MA 01731-5000	1
PHILLIPS LABORATORY PL LYP 3 HANSCOM AFB MA 01731-5000	1
US ARMY MATERIEL SYST ANALYSIS ACTIVITY AMXSY ATTN MR H COHEN APG MD 21005-5071	1
US ARMY MATERIEL SYST ANALYSIS ACTIVITY AMXSY AT ATTN MR CAMPBELL APG MD 21005-5071	1
US ARMY MATERIEL SYST ANALYSIS ACTIVITY AMXSY CR ATTN MR MARCHET APG MD 21005-5071	1
ARL CHEMICAL BIOLOGY NUC EFFECTS DIV AMSRL SL CO APG MD 21010-5423	1
US ARMY MATERIEL SYST ANALYSIS ACTIVITY AMSXY APG MD 21005-5071	1
ARMY RESEARCH LABORATORY AMSRL OP CI SD TL 2800 POWDER MILL ROAD ADELPHI MD 20783-1145	1
ARMY RESEARCH LABORATORY AMSRL SS SH ATTN DR SZTANKAY 2800 POWDER MILL ROAD ADELPHI MD 20783-1145	1

ARMY RESEARCH LABORATORY AMSRL IS ATTN J GANTT 2800 POWDER MILL ROAD ADELPHI MD 20783-1197	1
ARMY RESEARCH LABORATORY AMSRL DD ATTN J ROCCHIO 2800 POWDER MILL ROAD ADELPHI MD 20783	1
NATIONAL SECURITY AGCY W21 ATTN DR LONGBOTHUM 9800 SAVAGE ROAD FT GEORGE G MEADE MD 20755-6000	1
US ARMY RSRC OFC ATTN AMXRO GS DR BACH PO BOX 12211 RTP NC 27009	1
DR JERRY DAVIS NCSU PO BOX 8208 RALEIGH NC 27650-8208	1
US ARMY CECRL CECRL GP ATTN DR DETSCH HANOVER NH 03755-1290	1
US ARMY ARDEC SMCAR IMI I BLDG 59 DOVER NJ 07806-5000	1
ARMY DUGWAY PROVING GRD STEDP MT DA L 3 DUGWAY UT 84022-5000	1
ARMY DUGWAY PROVING GRD STEDP MT M ATTN MR BOWERS DUGWAY UT 84022-5000	1
DEPT OF THE AIR FORCE OL A 2D WEATHER SQUAD MAC HOLLOMAN AFB NM 88330-5000	1
PL WE KIRTLAND AFB NM 87118-6008	1
USAF ROME LAB TECH CORRIDOR W STE 262 RL SUL 26 ELECTR PKWY BLD 106 GRIFFISS AFB NY 13441-4514	1

AFMC DOW WRIGHT PATTERSON AFB OH 45433-5000	1
US ARMY FIELD ARTILLERY SCHOOL ATSF TSM TA FT SILL OK 73503-5600	1
US ARMY FOREIGN SCI TECH CTR CM 220 7TH STREET NE CHARLOTTESVILLE VA 22448-5000	1
NAVAL SURFACE WEAPONS CTR CODE G63 DAHLGREN VA 22448-5000	1
US ARMY OEC CSTE EFS PARK CENTER IV 4501 FORD AVE ALEXANDRIA VA 22302-1458	1
US ARMY CORPS OF ENGRS ENGR TOPOGRAPHICS LAB ETL GS LB FT BELVOIR VA 22060	1
US ARMY TOPO ENGR CTR CETEC ZC 1 FT BELVOIR VA 22060-5546	1
SCI AND TECHNOLOGY 101 RESEARCH DRIVE HAMPTON VA 23666-1340	1
US ARMY NUCLEAR CML AGCY MONA ZB BLDG 2073 SPRINGFIELD VA 22150-3198	1
USATRADO ATCD FA FT MONROE VA 23651-5170	1
ATRC WSS R WSMR NM 88002-5502	1
ARMY RESEARCH LABORATORY AMSRL IS S INFO SCI & TECH DIR WSMR NM 88002-5501	1
ARMY RESEARCH LABORATORY AMSRL IS E INFO SCI & TECH DIR WSMR NM 88002-5501	1

ARMY RESEARCH LABORATORY AMSRL IS W INFO SCI & TECH DIR WSMR NM 88002-5501	1
DTIC 8725 JOHN J KINGMAN RD STE 0944 FT BELVOIR VA 22060-6218	1
US ARMY MISSILE CMND AMSMI REDSTONE ARSENAL AL 35898-5243	1
US ARMY DUGWAY PROVING GRD STEDP3 DUGWAY UT 84022-5000	1
USTRADOC ATCD FA FT MONROE VA 23651-5170	1
WSMR TECH LIBRARY BR STEWIS IM IT WSMR NM 88002	1
US MILITARY ACADEMY DEPT OF MATHEMATICAL SCIENCES ATTN MDN A MAJ DON ENGEN THAYER HALL WEST POINT NY 10996-1786	1
ARMY RESEARCH LABORATORY AMSRL IS EW ATTN MR PASSNER WSMR NM 88002-5501	1
Record copy	1
TOTAL	67